Al-Juboori, G., Doufexi, A., & Nix, A. (2016). System level 5G evaluation of GFDM waveforms in an LTE-A platform. In 2016 International Symposium on Wireless Communication Systems (ISWCS 2016): Proceedings of a meeting held 20-23 September 2016, Poznan, Poland. (pp. 335-340). Institute of Electrical and Electronics Engineers (IEEE). DOI: 10.1109/ISWCS.2016.7600925

System Level 5G Evaluation of GFDM Waveforms in an LTE-A Platform

Ghaith R. Al-Juboori, Angela Doufexi and Andrew R. Nix

Communication Systems & Networks Group, Department of Electrical and Electronic Engineering
University of Bristol, Bristol, United Kingdom

Email: {Ghaith.Al-juboori, Angela.Doufexi, Andy.nix}@bristol.ac.uk

***Abstract* − 5G cellular systems must deliver high data rates, ultra-low power consumption and low end-to-end latency. Currently there is considerable interest in the design and performance of new 5G physical layer waveforms. One of the leading candidates is Generalized Frequency Division Multiplexing (GFDM). 5G waveforms are required to support a smooth transition from existing 4G solutions. In this paper the performance of a GFDM waveform is analysed in the context of LTE-A using the 3D 3GPP-ITU channel model. Results are directly compared with traditional OFDM solutions. Our analysis shows that GFDM achieves comparable Packet Error Rate (PER) and throughput results while introducing additional benefits such as reduced out-of-band radiation which is the key factor for the 5G cognitive applications based on dynamic spectrum access. We conclude that GFDM is a strong candidate for use in future 5G systems.**

***Index Terms* − GFDM; OFDM; LTE-A.**

I. INTRODUCTION

5G system requirements vary depending on the scenario, such as Machine Type Communications (MTC), Internet of Things (IoT) and mobile communications [1]. To achieve these requirements a variety of technologies need to be deployed, so as Massive Multi-User MIMO, millimetre wave communications and new physical layer waveforms. The choice of physical layer waveform is key since it impacts system level performance and transceiver complexity.

Orthogonal Frequency Division Multiplexing (OFDM) is used effectively as an air interface technique in many wireless standards. Examples include Digital Audio Broadcasting (DAB), Digital Video Broadcasting for Terrestrial Television (DVBT), Wireless Local Area Networks (WLAN 802.11 family) and 4G cellular (LTE-A). OFDM has many desirable features, such as robustness to Inter Symbol Interference (ISI) via low complexity equalisation. This is achieved by combining a Cyclic Prefix (CP) with Frequency Domain Equalisation (FDE). Waveform processing is further reduced by the efficient use of IFFT/FFT processing [2]. However, OFDM is known to suffer from several disadvantages [3]:

- High out-of-band emissions require an addition filter to fit within the regulatory spectral mask.
- High sensitivity to carrier frequency offset requires complex synchronisation to preserve orthogonality.
- Reliance on a CP reduces bandwidth efficiency.
- OFDM waveforms suffer from a high Peak to Average Power ratio (PAPR) that constrains amplifier design.

Recent research has proposed enhancements and alternatives to the OFDM waveform. The goal is to deliver the 5G requirements by implementing a waveform that is simple to transmit and receive, is robust to frequency offset and hardware impairments, offers good localisation in time and frequency and easily extends to embrace MIMO signal processing. In [4] the authors propose enhancements to the OFDM waveform to improve on many of its properties, such as spectral contamination and sensitivity to carrier frequency offset. Other work has suggested to replace OFDM with new waveforms such as the recently proposed GFDM, Filter Bank Multi-Carrier (FBMC)[5], Universal Filtered Multi-Carrier (UFMC) [6] and Bi-orthogonal Frequency Division Multiplexing (BFDM) [7]. In this paper, we focus on analysing the system level performance of GFDM and OFDM waveforms. Importantly, we compare simulated results for a multi-cell LTE-A like 5G deployment.

The remainder of this paper is organised as follows: Section II provides a brief description of the GFDM waveform, its key benefits and the transceiver model. Section III lists the LTE-A related system model parameters for OFDM and GFDM, while in Section IV the simulation results are presented and discussed. Finally, conclusions are given in section V.

II. GFDM SYSTEM MODEL

A. GFDM Overview

GFDM is a multicarrier modulation scheme with sufficient flexibility to address the requirements of 5G. The structure of the GFDM transmitter is shown in Fig. 1.

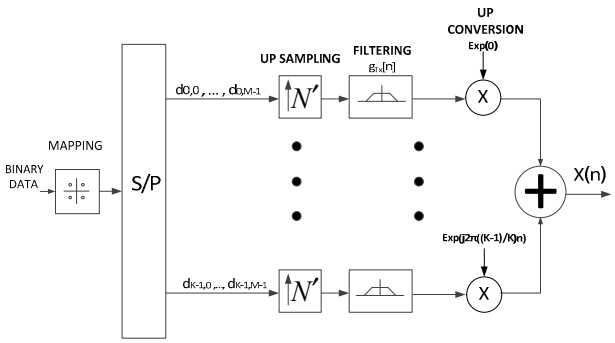

Fig.1: The basic structure of the GFDM transmitter.

Unlike OFDM, GFDM transmits *M* symbols per sub-carrier and the sub-carrier signal is oversampled by *N*', where $N' \geq K$ and *K* represents the number of sub-carriers. A pulse-shaping filter is then applied to each sub-carrier prior to up-conversion. The sub-carrier signals are added together to form the final waveform. A number of methods are reported in [3] to simplify the implementation of GFDM.

The GFDM block consists of *K* subcarriers and a number of sub-symbols *M*. The pulse-shaping process is used to filter each sub-carrier and this reduces the degree of Out-Of-Band (OOB) radiation [1]. Possible filters include the Raised Cosine (RC) filter, the Root Raised Cosine Filter (RRC) and the Dirichlet filter. The flexibility of the GFDM system stems from the use of non-orthogonal filters, as well as orthogonal filters [8]. As discussed in [1], the OOB radiation in the case of GFDM is around 15dB lower than OFDM. This difference can be further increased by inserting Guard Symbols (GS) and by pinching the Block Boundary[1]. Furthermore, GFDM has sharper spectral edges (i.e. reduction of OOB) in comparison to OFDM, however this requires a higher transmit and receive filter length. This length represents a problem due to its impact on the CP length, as shown mathematically in (1), where $L_{CP}, L_{channel}, L_{Tx\,F}$ & $L_{Rx\,F}$ denote the length of the CP, channel, transmit and receive filters respectively. This equation is necessary when effective FFT-based block equalisation is applied [8].

$$L_{CP} = L_{Tx\,F} + L_{channel} + L_{Rx\,F} \tag{1}$$

The tail biting technique (which considers circular rather than linear convolution between the signal and the impulse response of the filter) can be applied at the transmitter and receiver to reduce the CP length and achieve parity with the CP-OFDM case [8].

B. GFDM Transceiver

We consider the baseband GFDM transceiver as in [1]. First, a data vector ($\vec{b}$) is supplied to the encoder by the data source to produce the encoded data vector ($\overrightarrow{b_c}$). A signal mapper is used to map groups of μ encoded bits to their corresponding symbol, where μ represents the bits per symbol of the chosen modulation scheme. The resulting vector ($\vec{d}$) represents a data block containing *N* symbols that can be decomposed into *M* sub-symbols and *K* sub-carriers as below.

$$\overrightarrow{d} = \left(\vec{d}_o{}^T, \dots\dots\dots, \vec{d}_{M-1}{}^T\right)^T \tag{2}$$

$$\text{where} \quad \vec{d}_m = \left(d_{o,m}, \dots\dots\dots, d_{K-1,m}\right)^T \tag{3}$$

Each individual symbol $d_{k,m}$ represents the data symbol to be sent on the k^{th} sub-carrier and the m^{th} sub-symbol of the GFDM block. Fig. 2 shows the GFDM modulator, where each symbol ($d_{k,m}$) is filtered with its corresponding pulse shape as defined by (4).

$$g_{k,m}[n] = g[(n - mK) mod N] e^{-j2\pi \frac{k}{K} n} \tag{4}$$

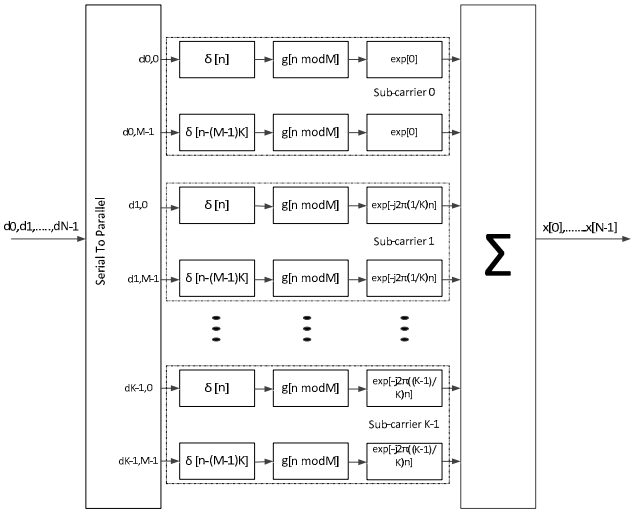

Fig.2: GFDM modulator [1].

where *n* is the sampling index and $g_{k,m}$ represents the time and frequency shift of the impulse response of the prototype filter. The resulting transmit samples can be expressed as

$$x[n] = \sum_{k=0}^{K-1} \sum_{m=0}^{M-1} g_{k,m}[n] d_{k,m} \tag{5}$$

where n=0, … , N-1. The above equation can be rewritten as

$$\vec{x} = A\vec{d} \tag{6}$$

where *A* represents the transmitter matrix with dimensions of $KM \times KM$ and its structure is given by [1]

$$A = \left[\overrightarrow{g_{0,0}} \dots\dots \overrightarrow{g_{k-1,0}} \overrightarrow{g_{0,1}} \dots\dots\dots\dots \overrightarrow{g_{k-1,m-1}}\right] \tag{7}$$

The wireless channel impulse response *h[n]* is assumed to be equal or less than the CP length. Moreover, perfect synchronisation and channel state information is assumed at the receiver. The received waveform after removing the CP can be expressed as

$$y[n] = x[n] \circledast h[n] + w[n] \tag{8}$$

where $w[n]$ represents the AWGN with zero mean and σ^2 variance. $\circledast$ refers to circular convolution with respect to n and periodicity *N*. Equalisation in the frequency domain is then performed as

$$\hat{x}(n) = F^{-1}\left[\frac{F(y[n])}{F(h[n])}\right] \tag{9}$$

where *F* represent the Discrete Fourier Transform (DFT). GFDM demodulation in the receiver and can be expresses as

$$\hat{d} = B.\hat{x} \tag{10}$$

where *B* is the GFDM demodulation matrix. Different linear methods can be used such as the Matched Filter receiver (MF), the Zero-Forcing receiver (ZF) and the Minimum Mean Square Error receiver (MMSE). In this paper, due to its simplicity compared to the MMSE approach, we use the ZF receiver, in

which $B = A^{-1}$. It should be noted that the ZF performance loss due to noise enhancement is zero due to the use of an orthogonal Dirichlet pulse [9].

III. SIMULATION PARAMETERS

A. LTE-A parameters

In this paper we develop a 20 MHz FDD LTE-A downlink simulator. The parameters of the LTE-A system are summarised in Table I [10]. The *standard mode* for LTE-A is used here where the CP length for the first and subsequent OFDM symbols is 160 and 144 samples respectively.

TABLE I: LTE-A PARAMETERS

Parameter	Value
Sub-frame duration	1ms or 30,720 samples
Slot duration	0.5 ms
Subcarrier spacing	15kHz
Sampling Frequency (clock)	30.72MHz
Number of subcarriers	2048
Number of active sub-carriers	1200
Resource block	12 subcarriers of one slot
Number of OFDM per sub-frame	14 (7 per time slot)
CP length-First symbol	160
CP length-Other symbols	144
Channel coding	Turbo code
MCS modes	QPSK1/3, QPSK1/2, QPSK2/3, 16QAM1/2, 16QAM2/3, 16QAM4/5, 64QAM2/3, 64QAM3/4, 64QAM 4/5

TABLE II: GFDM PARAMETERS

Parameter	Value
Sub-frame duration	1ms or 30,720 samples
GFDM symbol duration	66.67µs or 2048 samples
Sub-symbol duration	4.17µs or 128 samples
Subcarrier spacing	240 kHz
Sampling frequency	30.72 MHz
Subcarrier spacing factor (K)	128
No. of active subcarriers (K_{on})	75
No. of Sub-symbols per GFDM symbol (M)	15
No. of GFDM per sub-frame	15
CP length	4.17µs or 128 samples
Prototype filter	Dirichlet

B. GFDM parameters compatible to LTE-A

In order to use the GFDM waveform in the LTE-A grid, the symbol duration of the GFDM system must be selected to be an integer fraction of the LTE-A sub-frame period (1 ms) and a set of its sub-carriers must fit into an integer number of LTE resource blocks (1 Recourse block=180kHz). The GFDM parameters in [9] are used here, as shown in Table II. The channel coding and MCS parameters are taken from Table 1.

C. System-level parameters

Fig. 3 illustrates the 3GPP macro cellular deployment with a frequency reuse factor of one. Each cell consists of three sectors with cell radius, cell diameter and Inter Site Distance (ISD) of R, $2R$ and $3R$ respectively [11].

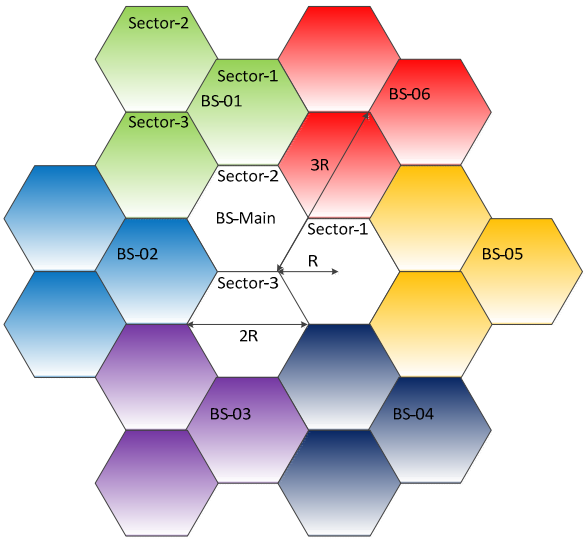

Fig. 3: Cell layout using 3GPP – 3-sector site.

TABLE III: SYSTEM LEVEL PARAMETERS

Parameter	Value
Channel model	Extended 3D 3GPP-ITU channel model
PDSCH simulation model	Bit level Simulator
Bandwidth	20 MHz
Carrier Frequency	2.6 GHz
Environment	Urban-Macro
Main BS-UEs distance	50 - 1000 m
Cell Diameter	500 m
BS transmit power	43 dBm
No. of users per cell	900
BS antenna height	25 m
BS down tilt	10 º
Minimum user sensitivity	-120 dBm
Link direction	Downlink (from BS to UE)
Noise Figure	9 dB
BS antenna type	Measured patch antenna as in [12]
UE antenna type	Measured hand set antenna as in [12]

The UEs were randomly distributed at street level in the cell, at a distance of between 50-1000m from the main BS. An operating frequency of 2.6 GHz and a bandwidth of 20MHz was assumed. The 3D 3GPP-ITU channel was applied, where the effect of elevation is also considered [13]. The system level parameters are summarised in Table III

To execute the system level analysis, bit level simulators for both waveforms (OFDM and GFDM) have been developed and used to calculate the PER for each user for 9 MCS modes. One thousand channel snapshots were produced for each link (between each UE and its serving BS and each UE and each one of six first-tier interfering BS) to generate statistically relevant performance data. The performance of both waveforms is studied for cases with and without interference. Table IV illustrates the MCS schemes and the maximum error free throughput for both waveforms.

TABLE IV: MCS AND R_{MCS} VALUES FOR BOTH WAVEFORMS

MCS-Number	No. of bit per symbol	R_c	OFDM-R_{MCS} in Mbps	GFDM-R_{MCS} in Mbps
MCS-1	2	1/3	11.2	11.25
MCS-2	2	1/2	16.8	16.875
MCS-3	2	2/3	22.4	22.5
MCS-4	4	1/2	33.6	33.75
MCS-5	4	2/3	44.8	45
MCS-6	4	4/5	53.76	54
MCS-7	6	2/3	67.2	67.5
MCS-8	6	3/4	75.6	75.94
MCS-9	6	4/5	80.64	81

In the interference-free case, only the effects of thermal noise need to be taken into account. The SNR is calculated as follows:

$$SNR_{i,M} = \frac{P_{i,Main}}{P_{AWGN}} \quad (11)$$

where $P_{i,Main}$ refers to the total received power at UE location i from the main BS sector cell and P_{AWGN} is the AWGN power. In the interference case, the interference comes from the different sectors of the six first-tier interfering BS. The SINR at each UE location is determined using (12)

$$SINR_i = \frac{P_{i,Main}}{P_{AWGN}+\sum_{ISI} P_{i,ISI}} \quad (12)$$

where $P_{i,ISI}$ refers to the total interference power at location i. Finally, the UE throughput is calculated using (13) [14]

$$THR_{i,MCS} = R_{MCS}\left(1 - PER_{i,MCS}\right) \quad (13)$$

where R_{MCS} is the peak error free data rate which represents the maximum data rate that can be transmitted without error for a given MCS mode.

IV. RESULTS

A. Comparison under different channel models

Fig. 4 shows the BER performance for both waveforms for 16QAM at a code rate of 1/3 in an AWGN channel.

Fig. 5 shows the performance of both waveforms in a narrowband Rayleigh fading channel. In general, for both waveforms the performance is much worse than AWGN. This is a result of dynamic fading and the lack of frequency diversity. Slightly worse performance is observed for GFDM since each sub-carrier consists of M modulation sub-symbols, while in OFDM each sub-carrier contains only a single symbol. Furthermore, an error across a particular subcarrier effects M symbols in GFDM rather than a single symbol in the case of OFDM; thus resulting in higher BER. However, this type of channels is very harsh and represents a theoretical case. The performance of the two waveforms at a certain UE location in a realistic urban channel scenario (3D 3GPP-ITU) is shown in Fig. (6) (K-factor of -9.7dB and delay spread of 0.12 micro second), it is clear that their performance are nearly matched and lower than the Rayleigh channel.

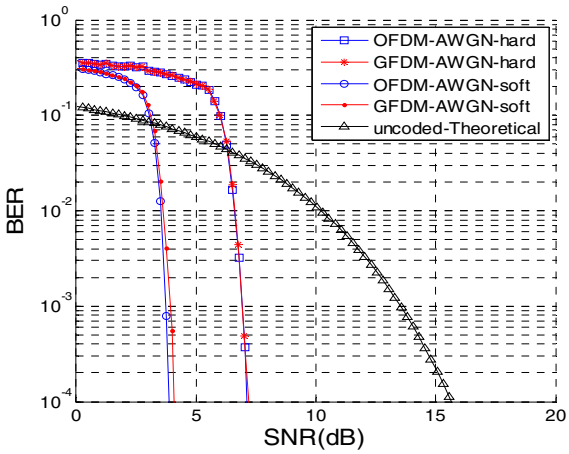

Fig. 4: Performance in AWGN channel.

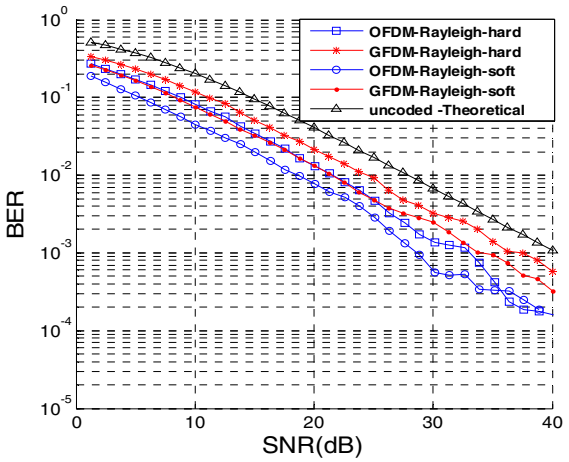

Fig. 5: Waveform performance in Rayleigh channel.

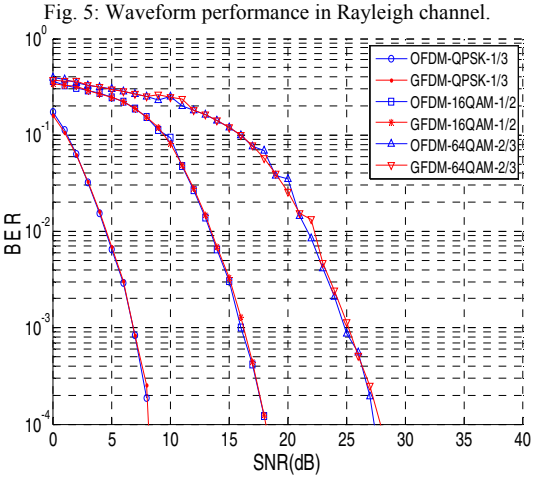

Fig. 6: Waveform performance in realistic channel scenario for certain UE.

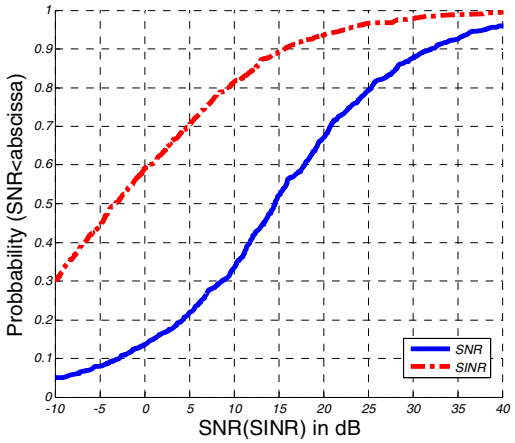

Fig. 7: Cumulative Distribution Function (CDF) for the UEs' SNR and SINR.

B. *System-level analysis*

Fig. 7 illustrates the Cumulative Distribution Function (CDF) of the UEs' SNR and SINR in the centre cell. We observe that 70% of the UEs' SNR values are equal to or less than 21 dB. When considering interference, 70% of the UEs' SINR values are equal to or less than 5 dB. The impact of interference is dramatic impact of interference. Importantly, the impact of interference can be reduced by methods such as beamforming [15].

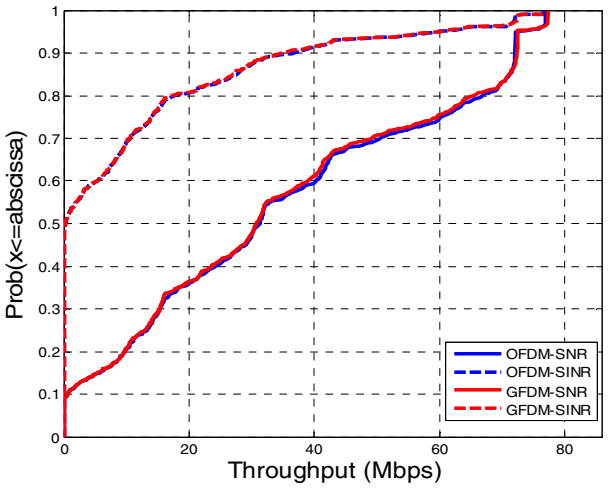

Fig. 8: CDF of Throughput using adaptive MCS selection.

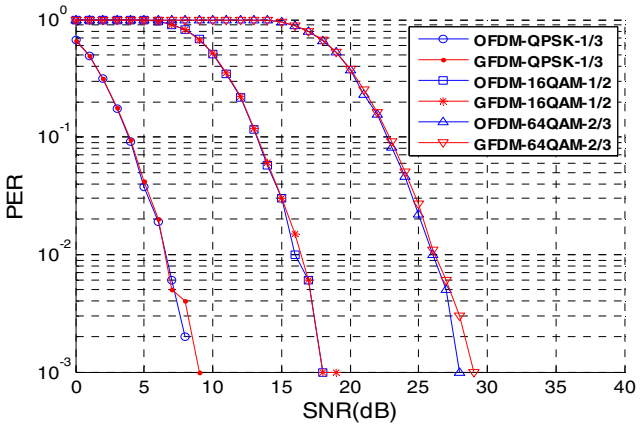

Fig. 9: PER vs SNR at an example UE location.

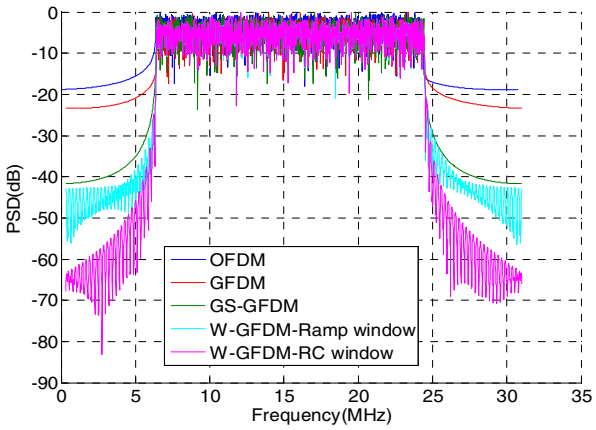

Fig. 10: Power Spectral Density (PDF) for GFDM and OFDM.

Fig. 8 shows the CDF for the PHY throughput; given the use of adaptive MCS selection (i.e. for each user the best MCS mode was selected using exhaustive simulation). We observe that the OFDM and GFDM results are very similar. The throughput for both schemes is clearly much better in the interference-free case. 65% of the UEs have a throughput greater than 20 Mbps in the interference-free case; while just 20% of the UEs achieve this rate when interference is considered in the simulator.

Fig. 9 shows an example of PER performance for a given UE location for MCS modes 1, 4 & 7. The aim is to compare the outcomes for GFDM and OFDM. The performance differences (based on a realistic urban channel model) are remarkably small compared to the earlier data for a simple Rayleigh fading channel.

Fig. 10 shows the Power Spectral Density (PSD) for both waveform types. GFDM results in a small reduction (approximately 6 dB) in the OOB radiation compared to OFDM. This modest reduction occurs since both waveforms have been constrained to deliver the same spectral efficiency (N_{cp}/N) [16]. However, as mentioned in section II-A, several methods can be used to significantly reduce the levels of OOB radiation.

In the Guard Symbols (GS) method, the first and last sub-symbols are set to a fixed value (zero in this study). This can result in approximately 20dB of improvement in OOB radiation, as shown in Fig. 9. However, this improvement comes at the cost of reducing the data rate by a factor of *(M-2)/M*. Secondly, pinching the block boundary, which implies multiplying the GFDM symbol with a window, leads to an OOB improvement of 25dB and 45 dB in the case of ramp and RC window schemes respectively. This method also enhances the noise by a factor of $(10 * log_{10}\left(1 + \frac{N_w}{K*M}\right))$, where N_w is the number of samples in the linear part of the window. Readers may refer to [1] for further details.

V. CONCLUSIONS

In this paper, the performance of GFDM and OFDM waveforms in an LTE-A like system was evaluated and

compared using different channel types. Also the system level analysis using a realistic channel model scenario (3D 3GPP-ITU) is evaluated and the simulation results have shown that the PER and throughput, for both waveforms, match closely. A modest improvement in the OOB radiation in case of GFDM in compared to OFDM is obtained, which is due to the fact the both waveforms (in this case) have the same spectral efficiency. However, the OOB radiation can be further enhanced for GFDM case compared to OFDM by using different methods like the guard symbols and pinching the block boundary. Although the GFDM provided comparable performance with OFDM in terms of BER, higher differences are expected in this context of OOB radiation when some LTE-A related physical parameters such as the sampling rate are adapted appropriately for the GFDM to fully utilise the benefit of this waveform. Hence we conclude that the GFDM waveform can be used effectively in future 5G systems. Since the GFDM exhibits reduced levels of OOB radiation in comparison to OFDM, this feature will enable GFDM to be used effectively in the applications where low adjacent channel leakage is required such as cognitive systems and M2M applications.

ACKNOWLEDGMENTS

Ghaith Al-Juboori would like to thank the Higher Committee for Education Development (HCED) in Iraq and the University of Baghdad for sponsoring his PhD studies.

REFERENCES

[1] N. Michailow, M. Matthe, I. S. Gaspar, A. N. Caldevilla, L. L. Mendes, A. Festag, *et al.*, "Generalized Frequency Division Multiplexing for 5th Generation Cellular Networks," *Communications, IEEE Transactions on,* vol. 62, pp. 3045-3061, 2014.

[2] L. L. Hanzo, Y. Akhtman, L. Wang, and M. Jiang, *MIMO-OFDM for LTE, WiFi and WiMAX: Coherent versus Non-coherent and Cooperative Turbo Transceivers* vol. 26: John Wiley & Sons, 2011.

[3] N. Michailow, I. Gaspar, S. Krone, M. Lentmaier, and G. Fettweis, "Generalized frequency division multiplexing: Analysis of an alternative multi-carrier technique for next generation cellular systems," in *Wireless Communication Systems (ISWCS), 2012 International Symposium on*, 2012, pp. 171-175.

[4] G. Berardinelli, K. Pajukoski, E. Lahetkangas, R. Wichman, O. Tirkkonen, and P. Mogensen, "On the Potential of OFDM Enhancements as 5G Waveforms," in *Vehicular Technology Conference (VTC Spring), 2014 IEEE 79th*, 2014, pp. 1-5.

[5] B. Farhang-Boroujeny, "OFDM Versus Filter Bank Multicarrier," *IEEE Signal Processing Magazine,* vol. 28, pp. 92-112, 2011.

[6] V. Vakilian, T. Wild, F. Schaich, S. t. Brink, and J. F. Frigon, "Universal-filtered multi-carrier technique for wireless systems beyond LTE," in *2013 IEEE Globecom Workshops (GC Wkshps)*, 2013, pp. 223-228.

[7] R. Ayadi, M. Siala, and I. Kammoun, "Transmit/receive pulse-shaping design in BFDM systems over time-frequency dispersive AWGN channel," in *Signal Processing and Communications, 2007. ICSPC 2007. IEEE International Conference on*, 2007, pp. 772-775.

[8] I. Gaspar, N. Michailow, A. Navarro, E. Ohlmer, S. Krone, and G. Fettweis, "Low Complexity GFDM Receiver Based On Sparse Frequency Domain Processing," *2013 Ieee 77th Vehicular Technology Conference (Vtc Spring),* 2013.

[9] I. Gaspar, L. Mendes, M. Matth, x00E, N. Michailow, A. Festag, *et al.*, "LTE-compatible 5G PHY based on generalized frequency division multiplexing," in *Wireless Communications Systems (ISWCS), 2014 11th International Symposium on*, 2014, pp. 209-213.

[10] 3GPP TS 36.211 V10.4.0, "Evolved Universal Terrestrial Radio Access (EUTRA):Physical Channels and Modulation," December 2011.

[11] 3GPP TS 36.942 V10.2.0, " Evolved Universal Terrestrial Radio Access (EUTRA):Radio Frequency (RF) System Scenarios," December 2010.

[12] R. Almesaeed, A. S. Ameen, A. Doufexi, and A. R. Nix, "Exploiting the elevation dimension of MIMO system for boosting handset capacity," in *2015 IEEE International Conference on Communication Workshop (ICCW)*, 2015, pp. 1281-1285.

[13] R. Almesaeed, A. S. Ameen, E. Mellios, A. Doufexi, and A. R. Nix, "A proposed 3D extension to the 3GPP/ITU channel model for 800 MHz and 2.6 GHz bands," in *Antennas and Propagation (EuCAP), 2014 8th European Conference on*, 2014, pp. 3039-3043.

[14] K. C. Beh, A. Doufexi, and S. Armour, "Performance Evaluation of Hybrid ARQ Schemes of 3GPP LTE OFDMA System," in *Personal, Indoor and Mobile Radio Communications, 2007. PIMRC 2007. IEEE 18th International Symposium on*, 2007, pp. 1-5.

[15] A. D. Panagopoulos, "Handbook of research on next generation mobile communication systems," 2016.

[16] A. B. U. a. A. O. Yilmaz. "Out-of-Band Radiation Comparison of GFDM, WCP-COQAM and OFDM at Equal Spectral Efficiency" arXiv preprint, Oct. 2015. [Online]. Available: http://arxiv.org/abs/1510.01201